Influence of oxygen deficiency on the superconductive properties of grain-aligned $YBa_2Cu_3O_{7-\delta}$

J. G. Ossandon*
Department of Physics, University of Tennessee, Knoxville, Tennessee 37996-1200

J. R. Thompson
Oak Ridge National Laboratory, Solid State Division, P.O. Box 2008, Oak Ridge, Tennessee 37831-6061
and Department of Physics, University of Tennessee, Knoxville, Tennessee 37996-1200

D. K. Christen, B. C. Sales, and H. R. Kerchner
Oak Ridge National Laboratory, Solid State Division, P.O. Box 2008, Oak Ridge, Tennessee 37831-6061

J. O. Thomson and Y. R. Sun
Department of Physics, University of Tennessee, Knoxville, Tennessee 37996-1200

K. W. Lay and J. E. Tkaczyk
General Electric Corporate R&D, Schenectady, New York 12301
(Received 17 September 1991)

Magnetically aligned samples of sintered $YBa_2Cu_3O_{7-\delta}$ were used to test the effects of oxygen-deficiency δ (with $\delta \leq 0.2$) on the superconductive magnetization M, critical current density J_c, irreversibility field B_{irr}, upper critical field H_{c2}, coherence length ξ, condensation energy F_c, penetration depth λ, and related properties as a function of temperature T and applied field $\mathbf{H}\|\mathbf{c}$. In selected cases, studies were also made with $\mathbf{H}\|ab$. The O content was monitored *in situ* by thermogravimetric analysis. The open porosity and granularity of the material allowed rapid and homogeneous oxygenation. We found no significant enhancement of intragrain J_c with chain-site O defects. With few exceptions, maximum J_c occurred at full oxygenation. This implies that chain-site O defects are not strong or effective pinning centers over most of the field-temperature regime investigated. Except for T_c, which was practically independent of δ within the interval $0 \leq \delta \leq 0.11$ (so called "90-K T_c plateau"), most properties such as J_c, F_c, H_{c2}, $B_{irr}(T)$, λ, and ξ were strongly and continuously influenced by the O deficiency. The observed abnormal magnetization with $\mathbf{H}\|\mathbf{c}$ was weak at low T but became more pronounced as T and δ increased. No abnormal magnetization was detected with $\mathbf{H}\|ab$. As oxygen was removed, $B_{irr}(T)$ and $H_{c2}(T)$ separated, and both lines shifted to lower T and lower B. Moreover, B_{irr} was strongly correlated with J_c at low temperature. Determination of the thermodynamic critical field H_c yielded condensation energies $F_c(\delta)$ that were well correlated with $J_c(\delta)$. The results indicate that O defects weaken the energy barrier of the existing pinning sites and have a negative overall effect on the capacity of $YBa_2Cu_3O_{7-\delta}$ to carry loss-free currents.

I. INTRODUCTION

Detailed effects of oxygen composition on the superconducting magnetic properties of $YBa_2Cu_3O_x$ are still not well understood due largely to the difficulty in controlling and varying the oxygen content of single crystals. Our purpose in this study was to investigate the properties of grain-aligned sintered samples of $YBa_2Cu_3O_x$ (hereafter Y 1:2:3) whose oxygen content, defined as $x=7-\delta$, could be easily varied and whose overall properties highly resembled those of single crystals.[1] Using standard experimental techniques and theoretical procedures, several magnetic superconductive properties were thoroughly measured for different values of δ within the range $0 \leq \delta \leq 0.2$. This composition range is of great practical significance since oxygen vacancies are always present in dense bulk material. The 90-K plateau of T_c for small δ is particularly interesting to examine because, while T_c is nearly constant in this interval, other properties may be strongly affected. We were especially interested in observing the "anomalous magnetization" phenomenon reported for Y 1:2:3 single crystals,[2] i.e., the presence of a "second peak" in the magnetization loop at higher fields. This phenomenon has been attributed to field-induced pinning at oxygen vacancies but its dependence on oxygen deficiency has not yet been systematically studied. More importantly, there is no clear understanding of the role that δ plays in the strength of preexisting pinning centers nor in the coupling between Cu-O planes.[3] A small oxygen deficiency may increase the pinning in high quality single crystals,[2] but its effect in thin films[4-6] and in randomly oriented polycrystalline material[7] is just the opposite. In this context there are many open questions, such as how are the condensation energy and the irreversibility line affected by δ? The present study provides answers to many of these questions and, in

particular, it shows that the overall effect of increasing oxygen deficiency is a monotonic decrease of J_c from its maximum value at full oxygenation. A simple, single-site pinning model helps explain this behavior. Although the "intrinsic" or "extrinsic" nature of some parameters is still a matter of discussion, the present study constitutes a significant contribution to these issues, of substantial theoretical and technological implications.[8]

II. EXPERIMENTAL ASPECTS

The sample synthesis has been described elsewhere.[1] A brief outline of the preparation technique is as follows. Previously prepared Y 1:2:3 powder was suspended in a solution of oleyl sarcosine and heptane and left to dry for 15 h in a 4-T magnetic field. The cake was removed from a mold and heated in flowing O_2 at a rate of 60 °C/h up to 840 °C. At this temperature it was maintained for 2 h to remove organic material. Portions of the cake were then sintered in flowing O_2 at 980 °C for 24 h and slow cooled (100 °C/h). After sintering, the pieces were sectioned with a diamond impregnated wheel and a wire saw, using ethanol or methanol as lubricants. Our sample was of cubic shape, of approximate dimensions $0.3\times0.3\times0.3$ cm^3, with the aligning field perpendicular to one face. Most of the Y 1:2:3 grains had their c axis aligned along the field direction, as verified by an x-ray-diffraction rocking curve FWHM of 7°. A small spot of silver epoxy indicated the c-axis face of the sample. The material was relatively porous; its bulk density was 5.0 g/cm^3, i.e., 78% of the theoretical x-ray density. The average grain radius was 7 μm and second phase impurities were negligible.

The oxygen content was systematically varied *in situ* using a thermogravimetric analysis (TGA) system. Prior to removing oxygen from the sample, a reference O content, $x=7$ (see below) was produced by first heating it to 500 °C in pure oxygen at a rate of 10 °C/min, then slowly cooling it back to room temperature at 2 °C/min. This provided the reference weight for the fully oxygenated sample from which changes in O content were calculated. Apparent changes in weight due to buoyancy effects were negligible. Prior to each subsequent modification of the O content, the sample was brought back to full oxygenation. The 100% oxygen atmosphere was then replaced with 99% Ar–1% O_2 mixture while the sample remained in the TGA system. The sample was heated to an appropriate temperature[9] between 370 and 470 °C, allowed to equilibrate overnight and then cooled rapidly to room temperature (200 °C/min), so that no significant change in the O content occurred (less than 0.01 O atoms per unit cell). The O content was calculated from the weight difference at room temperature of the oxygen-depleted sample and the O reference.

The heat treatment used to adjust the initial oxygen content to 7.00 ± 0.01 was determined using the careful and thorough equilibrium data of Lindemer *et al.*[9] According to this, the equilibrium oxygen content of Y 1:2:3 ceramic at an oxygen partial pressure of 1 atm is very close to 7.00 for temperatures between 300 and 350 °C (6.997 and 6.992, respectively). Lindemer's data are in good agreement with several other studies cited in his paper, and are much more precise than we could determine with our TGA apparatus by hydrogen reduction analysis, for example.

With the above procedure, the oxygen content of our sample was adjusted to 7.00, 6.89, 6.80, 7.00, 6.94, and 6.85, successively. These values were accurate to within ±0.01 oxygen atoms per unit cell, and remained stable over several weeks of magnetic measurements, as indicated by the sample weight. The sample used in this study had a mass of 160 mg, geometric volume 0.032 cm^3, and demagnetizing factor $D=0.34(\pm0.01)$ as determined from Meissner state measurements of magnetic moment versus applied field, directed along the edge of the cubical sample. (Strictly speaking, the concept of a scalar demagnetizing factor is applicable only to ellipsoidal samples with field applied parallel to a principal axis. We use D primarily for treatment of low field data with small or zero flux density in the sample. The value measured for our cubical sample, 0.34 ± 0.01, coincides within experimental error with other measurements on a lead cube in the Meissner state, and it plausibly agrees with the value $D=\frac{1}{3}$ for a sphere.)

Using a vibrating sample magnetometer (VSM), a SQUID magnetometer (Quantum Design MPMS), and an alternating current magnetometer (ACM), the following properties were measured or derived as functions of δ: critical temperature T_c, magnetization $M(H,T)$, critical current density $J_c(H,T)$, critical fields $H_c(T)$, $H_{c1}(T)$, and $H_{c2}(T)$; irreversibility line $B_{\rm irr}(T)$, condensation energy F_c, coherence length ξ, penetration depth eigenvalues λ_a and λ_c, anisotropy parameter γ, and others. The determinations are described in the following. Flux-creep measurements are in progress and are planned to be reported later.

III. EXPERIMENTAL RESULTS

A. Critical temperature T_c

Figure 1 shows the finite-field susceptibility, defined as $-4\pi M(T)/H_{\rm eff}$ (see below) as measured with the VSM in a small applied field ($H=10.8$ Oe), with $\mathbf{H}\|\mathbf{c}$ in all cases. The results correspond to five different oxygen contents: $x=7.00$, 6.94, 6.89, 6.85, and 6.80. In the zero-field-cooled (ZFC) study, the sample was cooled to 4.2 K with $H_{\rm app}=0$, after which the magnetizing field was applied; the resulting magnetization was measured as a function of temperature as the sample was slowly warmed to $T>T_c$. For the field-cooled history (FC), the sample was slowly cooled in the same applied field, during which the Meissner signal was measured. The ZFC and the FC signals were corrected for demagnetizing effects. As readily seen from the curves, the superconducting transition was sharpest for $x=7.00$ and broadest for $x=6.80$. The relative width of the transition $\Delta T/T_c$ increased with δ (where ΔT was defined as the temperature separation between the 10%- and the 90%-value of the magnetization signal). The results are tabulated in Table I.

Zero-onset T_c values, at which magnetic signals vanished, are shown in the inset of Fig. 1. They exhibit the well-known plateau pattern[10] with nearly constant T_c at

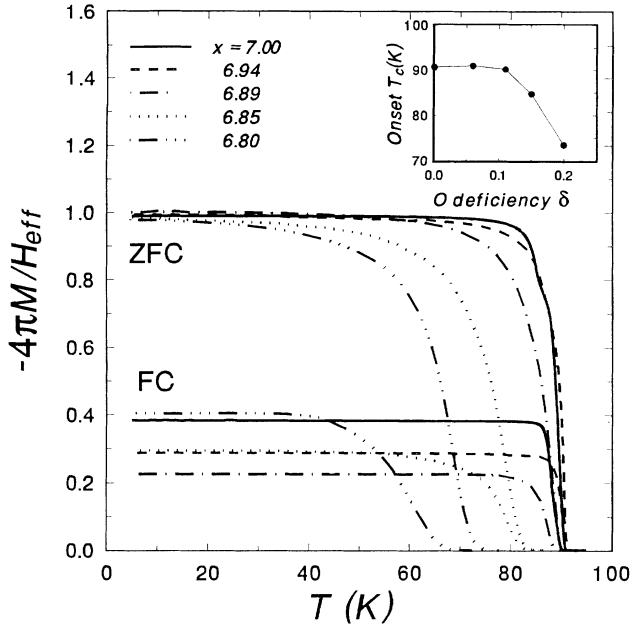

FIG. 1. Normalized dc magnetization $-4\pi M(T)/H_{\text{eff}}$ vs temperature of $YBa_2Cu_3O_x$ for zero-field-cooled (ZFC) and for field-cooled (FC) history in a small applied field $H\|c=10.8$ Oe. Zero-onset (threshold) T_c was nearly constant ("T_c plateau") for the first three samples (as shown in the inset).

≈ 90 K for $0\leq\delta\leq 0.11$, and decreasing T_c for $\delta\geq 0.11$. These VSM results agreed well with our ACM and MPMS measurements as well as with other previously published values.[11–13]

As an incidental further characterization of the materials, information on the "Meissner Fraction" is included in Table I. In particular, the ratio $r\equiv -4\pi M_{\text{FC}}/H_{\text{app}}$ at $T=4.2$ K is tabulated, with M_{FC} (field-cooled magnetization) based on the geometrical volume of the sample, as discussed below. Alternatively, one can include an approximate correction for demagnetizing effects. Since the effective field $H_{\text{eff}}\equiv H_{\text{app}}-4\pi DM$ depends on M, the ratio[14] between the FC and the ZFC susceptibilities at $T=4.2$ K, namely $[-4\pi M(0)/H_{\text{eff}}]_{\text{FC}}/[-4\pi M(0)/H_{\text{eff}}]_{\text{ZFC}}$, provides another measure of the Meissner state response; this is also tabulated in Table I.

In *this* case of small fields ($H\approx 10$ G) and surface screening currents, the FC and ZFC magnetizations were calculated as the induced-magnetic moment $m(T)$ divided by the *geometric* volume of the samples. Consequently, no account was made for the porosity of the material. Note, however, that in ZFC studies the entire geometrical volume of the sample was screened by the induced-surface currents. The sample with $\delta=0$ did not completely expel the magnetic flux when field cooled, but only a fraction of about 40%. This percentage decreased to slightly above 20% for $\delta=0.11$ and then increased back to more than 40% for $\delta=0.2$. Since the material was polycrystalline and porous, intergrain as well as intragrain properties were involved in the Meissner (FC) response, resulting in a complex overall behavior. Although the possibility of an effect on intergrain coupling by oxygen content may exist, there are too many uncertainties involved to draw a meaningful conclusion.

We turn now to the main subject of this paper, the *intragrain* properties of Y 1:2:3 and their dependence on oxygen deficiency δ. In all subsequent sections of this study, the experiments were performed in magnetic fields large enough to overcome completely intergrain coupling. Hence the aligned composite acted effectively as an array of independent single crystals.

B. Magnetic hysteresis

Magnetic hysteresis loops $M(H)$ in applied magnetic fields up to 6.5 T were measured in the VSM at fixed temperatures ranging from 4.2 to 70 K. In this and all following sections, the magnetization $M(T)$ refers to the measured magnetic moment $m(T)$ divided by the volume of superconductor as calculated from the sample mass and the theoretical density of 6.38 gm/cm^3. Typical results are shown in Figs. 2(a) and 2(b), corresponding to $T=4.2$ K and $T=30$ K, respectively, for various oxygen contents. Fields parallel to the c axis were applied at a sweeping rate of 108 G/s. Only "dynamic" values of the magnetization were recorded. This sweep rate for the magnetic field corresponds to imposing an internal electric field of approximately 10^{-9}–10^{-10} V/cm within a

TABLE I. Magnetically aligned $YBa_2Cu_3O_x$, critical temperature, and Meissner fraction for various oxygen contents[a] (with $H_{\text{app}}\|c=10.8$ Oe).

Oxygen content x	7.00	6.94	6.89	6.85	6.80
Zero-onset T_c (K)	90.7	91.0	90.2	84.7	73.5
10%-onset T_c (K)	89.7	90.3	87.9	80.4	68.2
Transition width ΔT (10–90%) (K)	6.8	10.0	16.7	24.8	25.7
$r\equiv -4\pi M_{\text{FC}}(0)/H_{\text{app}}$ (%)	44	32	24	33	47
$[-4\pi M(0)/H_{\text{eff}}]_{\text{FC}}/[-4\pi M(0)/H_{\text{eff}}]_{\text{ZFC}}$ (%)	40	30	22	31	41

[a]Values of x are accurate to within ± 0.01 atoms/cell; temperature measurements are accurate to within ± 0.1 K. Uncertainties in the magnetization and magnetic field determinations are typically of the order of ± 2–5 %.

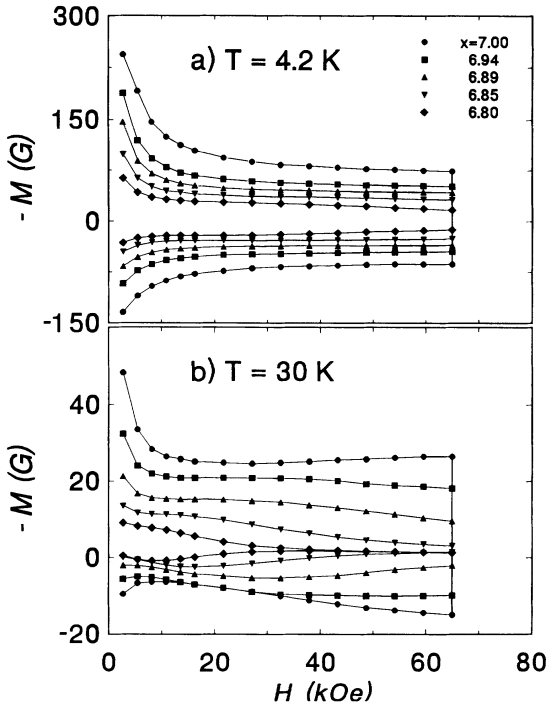

FIG. 2. Magnetic hysteresis loops of $YBa_2Cu_3O_x$ in applied fields $H \approx 0.3 \sim 6.5$ T, with $H \| c$ and H large enough to fully penetrate the Y 1:2:3 crystallites. (a) At $T = 4.2$ K, M decreased monotonically with H. (b) At higher temperatures, anomalous magnetization (increasing M with increasing H) was observed ("abnormal" effect).

crystallite, which is much lower than the typical criterion of 10^{-6} V/cm employed in transport studies. When the field sweep was halted periodically for about 20 s, the magnetization relaxed toward a "quasistatic" value due to flux creep, varying *approximately* logarithmically with time. (Recent studies on single crystals of Y 1:2:3 have revealed, however, significant departures from a truly logarithmic time dependence.[15]) Studies of flux creep as a function of oxygen deficiency will be reported elsewhere.

At low temperature ($T \leq 10$ K), the hysteresis curves appeared "normal," i.e., the magnetization signal decreased monotonically with increasing applied field, except for the least oxygenated sample ($x = 6.80$), which presented faint signs of "anomalous magnetization" or "abnormal" behavior.[2] At fields higher than one Tesla ($H \geq 1$ T), the magnetization M was practically independent of H for both increasing and decreasing field history. Most importantly, the hysteretic $M(H)$ decreased significantly as oxygen was removed; indeed, for all values of field recorded, the maximum magnetization occurred at full oxygenation ($x = 7.00$), falling by a factor of 2 at $x = 6.89$, and more than a factor of 4 at $x = 6.80$.

As the temperature increased, the hysteresis decreased as expected, but the shape of the curves changed dramatically. At $T = 30$ K [Fig. 2(b)] the absolute magnetizations decreased by one order of magnitude from the values at 4.2 K. Furthermore, all five curves exhibited the typical "abnormal" effect, i.e., increasing magnetization with increasing field within a certain field interval. An enhancement of $M(T)$ with increasing field ("anomalous magnetization") has also been observed in Y 1:2:3 single crystals,[2] but its quantitative dependence on oxygen content has not been well established. Concerning our grain-aligned samples, with H applied parallel to the c axis, the "anomaly" became clearly more pronounced (in relative terms) as T and δ increased. While the phenomenon may also occur with H perpendicular to the c axis, no "fishtail" was observed in our study with $\mathbf{H} \| ab$.

C. Critical current density J_c

Figures 3(a), 3(b), and 3(c) show the intragrain critical current densities $J_c(H)$ of the differently oxygenated samples for $H \| c$ at three fixed temperatures of 4.2, 40, and 60 K, respectively, for fields up to 6.5 T. They were determined from the magnetization curves using the Bean model[16–18,14] for spherical grains:

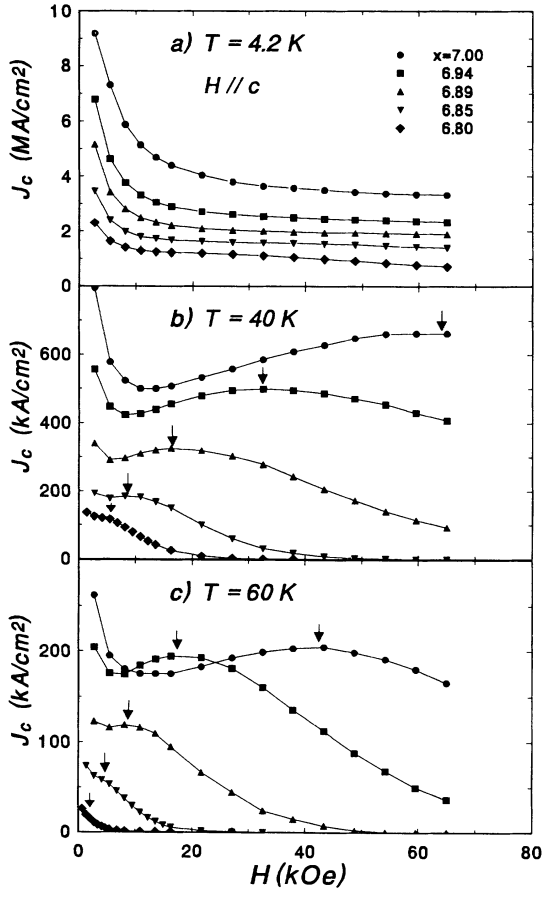

FIG. 3. Intragrain critical current density J_c vs applied field H for various oxygen compositions. (a) At $T = 4.2$ K, no J_c maxima were observed. Maximum J_c occurred at full oxygenation. (b) At $T = 40$ K, J_c was one order of magnitude lower than in (a) but secondary maxima were observed (indicated by the arrows). (c) The maxima became more pronounced as T and δ increased.

$$J_c = 16.9\Delta M/R \ , \quad (1)$$

where J_c is in A/cm^2, R(cm) = average grain radius,[19] and $\Delta M(G) = (M^- - M^+)$ = width of the hysteresis loop for increasing (M^+) and decreasing (M^-) field history. The actual grain morphology has been described in Ref. 1, and consists of platelike crystallites, whose average grain size was determined from optical micrographs. Since the same Y 1:2:3 specimen was used for all measurements, the relative features observed in M, J_c, etc., are independent of grain size, dispersion of grain size, and detailed morphology.

At 4.2 K [Fig. 3(a)] the $J_c(H)$ curves appeared "normal," i.e., they exhibited a monotonic decrease of J_c with H. Also, the highest J_c occurred at full oxygenation for all values of field measured. At this temperature, lower oxygen content clearly depressed the current-carrying capacity of the sample, having a negative impact on the pinning force density. The overall effect of higher oxygen deficiency was a monotonic decrease of J_c throughout the entire field range. This finding is fully in agreement with recent studies of oxygen vacancy effects on the flux pinning in high-J_c epitaxial thin films,[4-6] as well as in randomly oriented polycrystals.[7] However, it seems to contradict the proposition[2] that oxygen defects in Y 1:2:3 crystals act as significant pinning centers (for a discussion on this point, see Sec. IV).

At higher temperatures (up to 70 K), the critical current density $J_c(T)$ decreased with T as expected. However, the anomalous magnetization mentioned above gave rise to a nonmonotonic decay of J_c with H; instead of only one J_c peak (at $H=0$) a secondary peak emerged at higher field values. The position of this secondary peak (or "maxima") was highly dependent on oxygen deficiency and temperature. For example, at $T=40$ K [Fig. 3(b)] the fully oxygenated sample ($x=7.0$) reached a secondary peak of J_c at about 65 kG, while the less oxygenated sample ($x=6.8$) had a secondary peak at about 5 kG.

Another interesting feature of the J_c diagrams (with $\mathbf{H}\|\mathbf{c}$) at high temperatures is the crossing over the $x=7.0$ by the $x=6.94$ curve in the vicinity of $H=1.5$ T. Indeed, at $T=60$ K [Fig. 3(c)] we found a slight enhancement of $J_c(6.94)$ over $J_c(7.0)$ in a field interval between 1 and 2 T. This enhancement was more pronounced (in relative terms) at $T=70$ K, reaching a maximum of about 12% over the fully oxygenated sample, although the field interval of overlap was somewhat smaller.

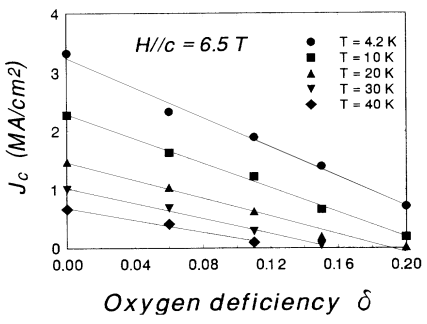

FIG. 4. J_c at $H=6.5$ T and fixed T (with $H\|c$) decayed linearly with δ at all temperatures, indicating a weakening of the pinning strength as oxygen was removed from the sample.

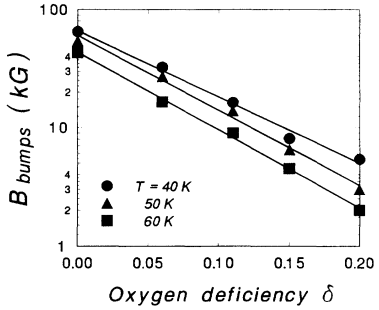

FIG. 5. The field position of the J_c maxima decreased nearly exponentially with increasing oxygen vacancies, as illustrated at three different temperatures.

The variation of J_c with δ at $H=6.5$ T (with $\mathbf{H}\|\mathbf{c}$) is shown in Fig. 4 for several temperatures between 4.2 and 40 K. It is seen that J_c decayed almost linearly with δ at all temperatures, being largest at full oxygenation. Unlike the transition temperature T_c, no "plateau" was found for $J_c(\delta)$.

The field positions of the J_c maxima observed in the different samples at various temperatures are shown in Fig. 5, with $\mathbf{H}\|\mathbf{c}$ in all cases. They shifted down as T increased; also, their δ dependence was well described by a negative exponential fit.

D. Irreversibility line $B_{irr}(T)$

A quick review of Fig. 3 indicates that, independent of temperature, the irreversibility point B_{irr} (where J_c vanishes) shifted to lower fields as oxygen was removed. This feature is corroborated in Fig. 6(a), which shows ac-response studies of the irreversibility lines $B_{irr}(T)$ in terms of the reduced temperature $t=T/T_c$. In this work, a field $H=H_{dc}+H_{ac}$ was applied along the c axis. The small ac-field amplitude $H_{ac}\approx 10$ G (frequency = 39 Hz) was chosen to produce a detectable "switching transient" response of the superconductor as the induced supercurrent reversed in direction of circulation. The irreversibility threshold was defined by the vanishing of the inductive transient voltage generated when the ac field switches M from the lower to the upper branch of the magnetization hysteresis loop. The transient voltage vanished, corresponding to $J_c=0$, when the dc field or temperature reached the irreversibility line from the hysteretic side. (This inductive technique differs somewhat from that often employed at higher frequencies, in which a very small amplitude ac field is used to map out the peak in ac loss that occurs near the irreversibility line.) Figure 6(a) indicates that the irreversibility line shifted down to lower field values as oxygen was removed from the material. The experimental data were fitted with a power law of the form

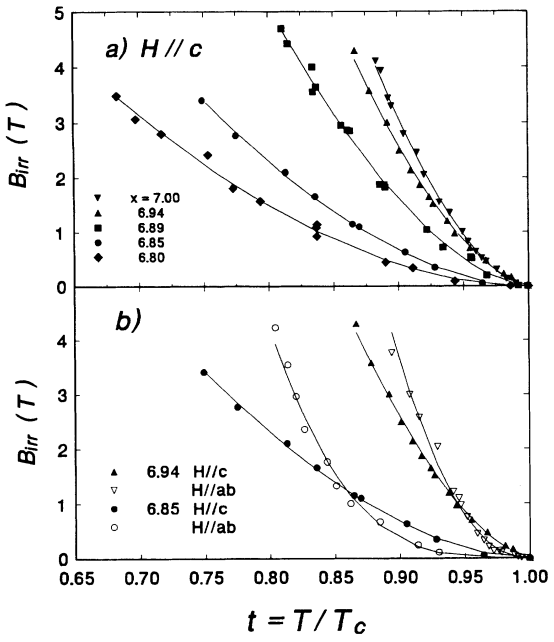

FIG. 6. (a) Irreversibility lines in terms of reduced temperature t: the lines shift down as oxygen content decreases; note that the three highest curves belong to samples with the same T_c value. (b) The irreversibility lines in two field orientations show for two samples a crossing of the lines at a field of about 1 Tesla. Solid curves are best fits to a power law $B_{irr}=B_0^*(1-t)^n$, with $n\approx 1.7$ for $H\|c$ and $n\approx 2.5$ for $H\|ab$.

$$B_{irr}=B_0^*(1-T/T_c)^n \ . \tag{2}$$

The best fits yielded $n=1.70(\pm 0.05)$ for all oxygen compositions. Using regression analysis, the parameter B_0^* was determined for each oxygen content and found to be strongly correlated with J_c. This striking correlation is treated in more detail in Sec. IV.

The depression of the irreversibility line brought about by chain-site oxygen defects is more than just an effect of T_c. In particular, the three highest curves ($x=7.0$, 6.94, 6.89) in Fig. 6(a) belong to samples with nearly the same T_c value. This result implies that the low-frequency irreversibility line cannot be considered as an "intrinsic" property of Y 1:2:3 (see Discussion, Sec. IV C). According to our measurements, the addition of chain-site oxygen defects lowers the irreversibility line, reduces the hysteretic region, enlarges the reversible ("vortex-fluid," "lattice-melted") region in the B-t plane, and overall hinders the capacity of Y 1:2:3 to carry intragrain loss-free currents at high fields and temperatures.

A very interesting feature of the irreversibility line is its anisotropy. Using the ACM in identical conditions, we measured $B_{irr}(T)$ with $\mathbf{H}\|\mathbf{c}$ and $\mathbf{H}\|ab$. The results for two different oxygen contents are depicted in Fig. 6(b). The fitted lines correspond to Eq. (2) with exponent $n\approx 1.7$ for $\mathbf{H}\|\mathbf{c}$ and $n\approx 2.5$ for $\mathbf{H}\|ab$. In both cases investigated, $B_{irr}(\mathbf{H}\|ab)$ was larger and exhibited a steeper slope than $B_{irr}(\mathbf{H}\|\mathbf{c})$ for field values above a crossing point of about 1 T, while the opposite was true for low-field values (in good agreement with recent low-field measurements in YBCO single crystals[20]).

E. Upper critical field $H_{c2}(T)$

To establish the influence of oxygen deficiency on the upper critical field $H_{c2}(T)$ was a crucial task in our study since several significant results follow from it. We approached the problem in two ways: first, we analyzed temperature-dependent magnetization data $M(T)$ using the linear extrapolation techniques of Welp *et al.*;[21] second, we followed the more analytical and complex procedure proposed recently by Hao *et al.*[22] In the following we report the results of both analyses and indicate similarities and differences.

The first estimates of the upper critical field of our sample for various oxygen compositions were derived from $M(T)$ measurements carried out with the SQUID magnetometer (for ZFC as well as FC history) at several fixed values of H in the reversible regime. Measurements were made over a temperature range from a few degrees below T_c to well above T_c in order to obtain the normal-state background. Following Welp *et al.*,[21] we employed a "linear analysis" to determine a nucleation temperature $T_c(H)$ as the intercept of a linear extrapolation of the reversible magnetization in the superconducting state with the normal-state base line. The resulting $H_{c2}(T)$ lines for various oxygen contents are shown in Fig. 7(a). Note that the $H_{c2}(T)$ lines are linear (as predicted by the

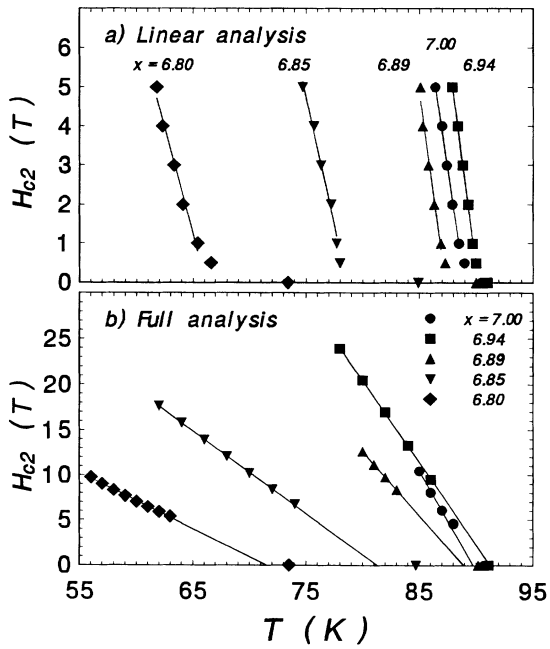

FIG. 7. H_{c2} lines near T_c of $YBa_2Cu_3O_x$ as determined from the linear analysis (a) and from the full analysis (b). Note that the two sets of points cover a different field range. Solid lines represent linear regressions fits to the data. Close to the horizontal axis, there are nonlinear "tails." Symbols on the temperature axis indicate zero-onset T_c values.

Ginzburg-Landau theory), except close to $T=T_c$, where there are nonlinear tails that have been attributed to diamagnetic fluctuations and sample inhomogeneities. Linear extrapolations of the H_{c2} lines intersect the horizontal axis a few degrees below the zero-onset T_c values of Table I, and closer to the 10%-onset T_c. The temperature difference increased as oxygen was removed. This same phenomenon was observed in the determination of the London penetration depth, as described below.

According to Werthamer, Helfand, and Hohenberg,[23] the upper critical field H_{c2} extrapolated to $T=0$ is proportional to the slope dH_{c2}/dT near T_c and is given by

$$H_{c2}(0)=0.7T_c\left[\frac{dH_{c2}}{dT}\right]_{\approx T_c} . \tag{3}$$

Applying this expression to the linear portion of the data for fields in the interval between 1 and 5 T (for temperatures above the irreversibility lines) provided first estimates of the upper critical fields H_{c2} at $T=0$, as a function of δ. The results are plotted in Fig. 8(a) (denoted "linear analysis") and tabulated in Table II. These estimates suggest that chain-site oxygen defects did not affect $H_{c2}(0)$ significantly for $\delta\leq 0.11$. With more oxygen defects, $H_{c2}(0)$ decreased rapidly.

The coherence lengths at $T=0$ were obtained from $H_{c2}(0)$ using the Ginzburg-Landau relationship:

$$H_{c2}=\Phi_0/(2\pi\xi_i\xi_j) , \tag{4}$$

where $\hat{i}$ and $\hat{j}$ denote two orthogonal unit vectors perpendicular to the applied field (which is assumed to lie along a principal axis). In the array of twinned crystals, we treated the system as uniaxial and ignored anisotropy within the basal *a-b* plane. Then, with $H\|c$, we have

$$H_{c2}=\Phi_0/2\pi(\xi_{ab})^2 \text{ with } \xi_{ab}\equiv\xi_a=\xi_b . \tag{5}$$

The calculated values for ξ_{ab} at $T=0$ are given in Table II ("linear analysis"). The value for the coherence length at full oxygenation (≈ 16 Å) agrees well with results reported by other researchers.[21,22] The value of $\xi_{ab}(\delta)$ was nearly constant for $\delta\leq 0.11$ and increased significantly to about 25 Å for $\delta=0.2$. This "plateau"-like behavior mirrored the $H_{c2}(0)$ findings of the linear analysis, of course.

Proceeding further with this technique, we investigated H_{c2} anisotropy. With $H\|ab$, the $M(T,H)$ signal in the superconducting state was about one order of magnitude smaller than with $H\|c$. Consequently, the slopes $dM(H)/dT$ near T_c were much more difficult to determine accurately and the values of $T_c(H)$ were somewhat ill defined. Nevertheless, a rough estimate of $-6.6(\pm 0.8)$ T/K for $(dH_{c2}/dT)_{\approx T_c}$ [as compared with $-1.3(\pm 0.04)$ T/K for $H\|c$] was obtained for one sample ($x=6.85$). The corresponding upper critical field $H_{c2}(0)$ was close to 400 T, which is roughly five times greater than the $H\|c$ estimate of 77 T. A more accurate measure of anisotropy using penetration depth eigenvalues is reported below.

The statistical uncertainty in $H_{c2}(0)$ associated with determinations of the slope dH_{c2}/dT was approximately 10%, corresponding to an uncertainty of $\sim 5\%$ in ξ. Of

TABLE II. Magnetically aligned $YBa_2Cu_3O_x$, characteristic fields, lengths, and parameters (with $H\|c$). The oxygen content x is accurate to within ± 0.01 atom/cell; temperature measurements are accurate to within ± 0.1 K. The statistical uncertainties in H_{c2}, dH_{c2}/dT, and H_{c1} are typically about 10–12 % while those in H_c are 3–5 %. The best fitting κ is defined to within 5–10 %. The uncertainties in ξ_{ab} and in λ_{ab} are about $\sim 5\%$, and in F_c about $\sim 8\%$.

Oxygen content x	7.00	6.94	6.89	6.85	6.80
Linear analysis:					
$H_{c2}(0)$ (T)	125	140	130	77	56
$(dH_{c2}/dT)_{\approx T_c}$ (T/K)	−2.0	−2.2	−2.1	−1.3	−1.1
$\xi_{ab}(0)$ (Å)	16.4	15.4	15.8	20.6	24.5
Full analysis:					
$H_{c2}(0)$ (T)	140	115	90	54	32
$(dH_{c2}/dT)_{\approx T_c}$ (T/K)	−2.2	−1.8	−1.4	−0.9	−0.6
$\xi_{ab}(0)$ (Å)	15.4	16.8	19.1	25.0	32.3
Best fitting $(\kappa)_{\approx T_c}$	77	78	84	72	66
$H_c(0)$ (kG)	10.7	9.1	6.5	4.7	3.0
$F_c(0)$ (J/cm^3)	0.45	0.33	0.17	0.09	0.04
$H_{c1}(0)$ (G)	370	320	210	180	120
$\lambda_{ab}(0)$ (nm)	140	150	190	200	240
T_{c,H_c} (K)	89.7	91.2	88.9	81.3	71.5
$M\sim\ln(H)$ analysis:					
$\lambda_{ab}(0)$ (nm)	160	170		230	
$T_{c,\lambda}$ (K)	90.5	90.6		78.7	

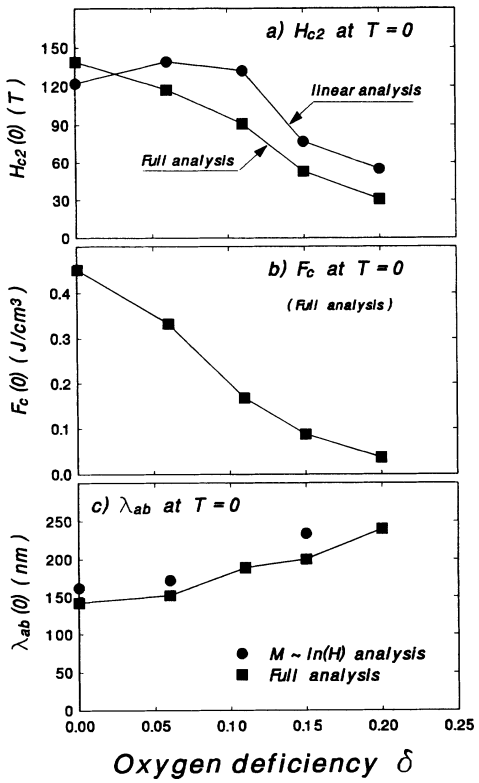

FIG. 8. (a) H_{c2} values as a function of δ extrapolated to $T=0$: the linear analysis suggests an "H_{c2} plateau" for $\delta \leq 0.11$ but the full analysis gives a continuous decrease with δ. (b) The condensation energy F_c at $T=0$, as derived from the full analysis, shows a significant decay with δ. (c) Penetration depth eigenvalues λ_{ab} calculated by two different techniques, increase steadily with δ. Error bars are of a size comparable to the symbols.

greater concern is the fact that this type of analysis is not consistent with the Ginzburg-Landau theory upon which it is based, as discussed in the next section. There we employ a recent theoretical analysis,[22] that is consistent with GL theory; the treatment is more numerical and less intuitive than that of Welp *et al.*, but much more reliable, in our opinion.

F. Thermodynamic critical field H_c and derived properties

Hao *et al.*[22] pointed out that much of the experimental magnetization data correspond to fields H far below $H_{c2}(T)$ and thus are not adequately described by the usual linear relation between M and H near $H_{c2}(T)$ which follows from Ginzburg-Landau theory.[24] Moreover, the observed field dependence in the slopes dM/dT (Ref. 21 and this work) confirms that the linearity between M and H is not a correct assumption. Consequently, a more complete theoretical treatment needs to be used. Following this line of thought, the experimental measurements discussed in the previous paragraph were reanalyzed according to the full theoretical analysis proposed by these authors.

Using the theoretical relationship of Hao *et al.*[22] that relates H to B by accounting for the kinetic-energy and the condensation-energy terms arising from the suppression of the order parameter in vortex cores (neglected in the usual London model), the diamagnetism $M(T,H)$ can be calculated numerically and fitted to the experimental data. From the fitting procedure, two significant properties are determined, namely, the Ginzburg-Landau parameter $\kappa(T) \equiv \lambda/\xi$ and the thermodynamic critical field $H_c(T)$. The product of these two gives $H_{c2}(T)=\sqrt{2}\kappa(T)H_c(T)$. Also $\lambda(T)$, $\xi(T)$, and $H_{c1}(T)$ can be obtained.

The fitting procedure, however, is not simple. For a fixed value of T within the reversible regime, the experimental values $-4\pi M_i/H_i$ have to be compared with the theoretical ratio $-4\pi M'/H'$ (where M' and H' are dimensionless quantities) as obtained from the simultaneous solution of Eqs. (20) and (21) of Ref. 22, with $B' \equiv H' + 4\pi M'$ and κ as adjustable parameters. Primes denote dimensionless units in which fields are measured in units of $\sqrt{2}H_c(T)$. The subindex i denotes values in different fields with T fixed. For each value of κ, there will be one solution B'. From this, M' and H' are derived. The unit of magnetic field is determined from $\sqrt{2}H_{ci}(T)=H_i/H'=M_i/M'$. This has to be done for each data point i. If the value chosen for κ is not "right," the resulting values for $H_{ci}(T)$ will not be constant (as they should be, since T is fixed). The best κ gives the minimum variance in the set of values for $H_{ci}(T)$. Figure 9 illustrates for one sample ($x=6.89$) the good agreement between magnetization data (symbols) and the theoretical model of Hao *et al.* (solid line) in the reduced (dimensionless) M'-H' plane for one value of the parameter κ. Unfortunately, this fitting technique is not very sensitive to κ, as variations of 5–10 % in the estimate of κ produces a smaller effect (about half as much) on the thermodynamic critical field value $H_c(T)$. Although $H_c(T)$ turns out to be relatively well defined (within 3–5 %), κ values are less sharply defined (typically within 5–10 %). This fact introduces an uncertainty of 8–15 % in the estimates of the upper critical field $H_{c2}(T)$.

In this analysis, another problem is an appropriate choice of the temperature range, which must be not too far below T_c, since the system must be reversible, but not

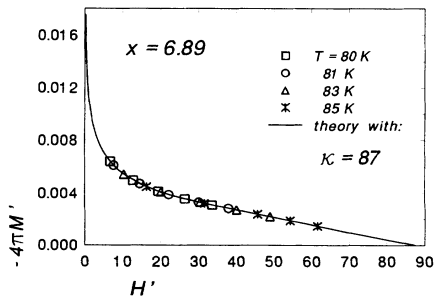

FIG. 9. Nearly perfect agreement between the magnetization data and the theoretical model of Hao *et al.* (Ref. 22) for $\kappa=87$ in the $x=6.89$ sample.

too close to T_c either, where the Ginzburg-Landau mean-field theory becomes invalid. Near T_c, κ should be constant, but in practice the "best" κ values increase with temperature, accelerating upward and reaching apparent values of 150 or 200 in the fluctuation region near T_c. Therefore, the most suitable temperature range should be that for which the parameter κ shows the smallest temperature dependence.

Once the temperature-dependent values for $H_c(T)$ were determined for each composition (in the $H\|c$ orientation), the values $H_c(0,\delta)$ at $T=0$ were obtained by a fitting process, using the BCS temperature dependence[25] of $H_c(T)$. On the other hand, the $H_{c2}(T)$ lines near T_c were constructed from $H_c(T)$ and κ; they are shown in Fig. 7(b) (denoted "full analysis"). Their extrapolations to zero field intersect the horizontal axis at the values labeled T_{c,H_c}, as tabulated in Table II. Finally, since the T dependence of κ was not known, we obtained the $H_{c2}(0)$ values of each sample by WHH extrapolation using Eq. (3). The different extrapolation criteria for H_c and H_{c2} are consistent with the fact that the Ginzburg-Landau parameter κ is temperature dependent.[26] The results are given in Table II and plotted in Fig. 8(a) ("full analysis"). Unlike the results from the linear analysis, both $H_c(0)$ and $H_{c2}(0)$ decreased monotonically as the material became less oxygenated; there was no "plateau" in the δ dependency. The magnitudes of the upper critical fields calculated from the full analysis were lower (except for the $x=7.00$ sample) than the estimates from linear extrapolation techniques. The corresponding coherence lengths $\xi_{ab}(0)$ are also tabulated in Table II.

The above determination of the thermodynamic critical field H_c allowed us to evaluate the condensation energy density $F_c=H_c^2/8\pi$ for various oxygen constants. To avoid temperature effects, we restricted ourselves to ($T=0$) values. We found that $F_c(0)$ strongly decreased with increasing oxygen deficiency, in a manner that highly resembled the behavior of J_c [Fig. 8(b)]. Finally the derived quantities $\xi_{ab}(0)$ and $H_{c1}(0)$ were readily calculated from $\kappa(0)$, $H_c(0)$, and $H_{c2}(0)$, and are tabulated in Table II.

G. London penetration depth λ_{eff}

To characterize further the influence of oxygen deficiency on the properties of Y 1:2:3 superconductor, we determined the magnetic penetration depth λ at $T=0$ of the samples in two alternative ways: (1) using the already established results (as obtained from the full analysis) for $H_c(0)$ and $\xi_{ab}(0)$ via

$$\lambda(0)=\phi_0/[2\sqrt{2}\,\pi H_c(0)\xi_{ab}(0)] \tag{6}$$

and (2) following the theoretical analysis of Kogan *et al.*[27] which provides a linear relation between M and $\ln(H)$ in the intermediate field region of the reversible magnetization curves near T_c. In particular, the London penetration depth $\lambda_{\text{eff}}(T)$ with $H\|c$ was measured for the $x=7.00$, 6.94, and 6.85 compositions following Kogan's technique. Then, $\lambda_{\text{eff}}(0)$ was obtained by fitting BCS-clean limit theory to the experimental values. We also measured $\lambda_{\text{eff}}(0)$ with $H\|ab$ for the $x=6.94$ and 6.85 samples, in order to evaluate the anisotropy parameter $\gamma^2\equiv m_c/m_a$, as described below.

According to Kogan *et al.*[27]

$$[\lambda_{\text{eff}}(T)]^2=\phi_0\Big/\left[32\pi^2\frac{dM}{d(\ln H)}\right]. \tag{7}$$

This relation is valid in the field range $H_{c1}\ll H\ll H_{c2}$ when the magnetization is reversible, and applies to uniaxial materials. As before, we ignore any anisotropy within the basal a-b plane.

Figure 10 shows M plotted versus $\ln H$ for three oxygen compositions, where M is the net, reversible magnetization corrected for background. Linear regression lines were fitted to the data to obtain the logarithmic slope $dM/d(\ln H)$ and the effective penetration depth $\lambda_{\text{eff}}(T)$ using Eq. (7).

For comparison purposes we were interested in λ_{eff} at $T=0$. To find it, we determined first the magnetic transition temperature $T_{c,\lambda}$ at which λ_{eff} diverges, or $1/\lambda_{\text{eff}}$ extrapolates to zero. Near T_c, Ginzburg-Landau theory

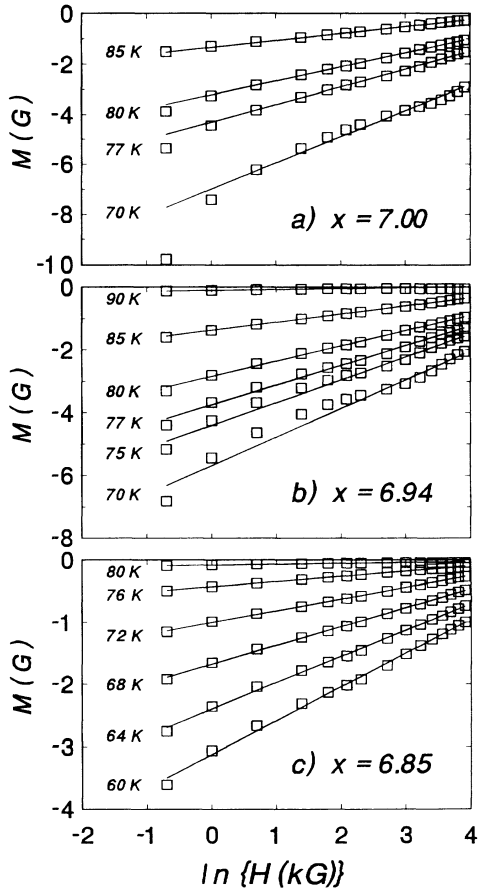

FIG. 10. Magnetization data for three oxygen compositions show a good linear relation with $\ln(H)$ in the reversible region near T_c, as predicted by the theoretical model of Kogan *et al.* (Ref. 27). Linear regression fits (solid lines) yield the effective penetration depths as functions of T.

provides a linear relation between $(1/\lambda_{\rm eff})^2$ and $(T_c - T)$. We obtained values for $T_{c,\lambda}$ by extrapolating such a linear plot to the point that $(1/\lambda_{\rm eff})^2 = 0$. Then we fitted BCS-clean limit theory for $[\lambda(0)/\lambda(t)]^2$ to the experimental values of $[1/\lambda_{\rm eff}(t)]^2$, as indicated in Fig. 11 for one sample ($x = 6.94$) and two orientations. Previous work[28–31] has shown that this theory provides a good description of the temperature dependence of λ in many families of high-T_c superconductors. With $T_{c,\lambda}$ already established, the only fitting parameter left was $\lambda_{\rm eff}(0)$. Results are reported in Table II and plotted in Fig. 8(c) for comparison with values obtained from the full analysis. The latter values for λ were consistently (about 12%) lower than those from the $M \sim \ln H$ analysis. This difference was predicted and shown by Hao and Clem[32] to arise from a neglect of vortex core contributions to the free energy in the mixed state. Since the values obtained from both analyses were nearly proportional, they followed a similar pattern with respect to oxygen deficiency: as δ decreased, $\lambda(\delta)$ also increased.

Before proceeding, it is worth mentioning that the magnetic transition temperatures $T_{c,\lambda}$ of the samples [as obtained from the $M \sim \ln H$ analysis where $(1/\lambda_{\rm eff})^2 \rightarrow 0$] agreed well with the 10%-onset values for T_c as listed in Table I. In some cases of sharp transition, e.g., $x = 7.00$ and 6.94, they also coincide well with the zero-onset value. However, in the case of the 6.85-sample ($\delta = 0.15$), the value of $T_{c,\lambda}$ (for $H \| c$ as well as for $H \| ab$) was about 5 K less than the zero-onset value of 84.7 K. It appears that the following set of transition temperatures is consistent to within ± 1–2 K for any given composition: (1) 10%-onset T_c in low field; (2) $T_{c,\lambda}$ as obtained from the $M \sim \ln H$ analysis; and (3) T_{c,H_c} from extrapolation of $H_c(T)$ or $H_{c2}(T)$ to zero field in the full analysis.

Indeed the experimental curve $(1/\lambda_{\rm eff})^2$ versus T for the 6.85-sample showed clear departure from the Ginzburg-Landau linear relation close to T_c. This behavior, which was connected with the fact that this sample had a much broader superconducting transition as compared with the two previous ones, suggests that the narrow temperature domain $T_{\rm GL} < T < T_c$ where the mean-field theory is no longer valid, may increase with the oxygen deficiency. Moreover, very near to T_c some departure from the theory is expected since the application of large fields in the λ determination violates the assumption that $H \ll H_{c2}$. These factors, together with sample inhomogeneities and diamagnetic fluctuations, explain the observed tails on the transition.

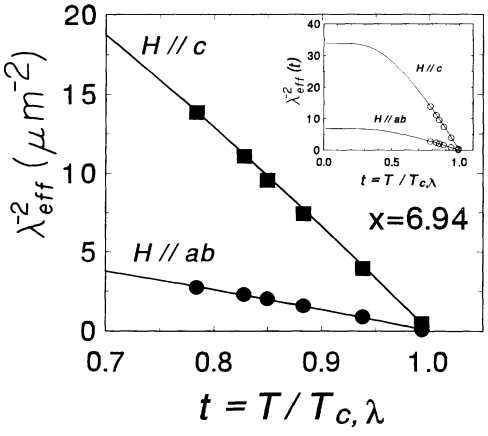

FIG. 11. Fitting of the BCS-clean limit theory to $[1/\lambda_{\rm eff}(t)]^2$, where $t = T/T_{c,\lambda}$, allows an evaluation of the effective penetration depths at $T = 0$. The full BCS extrapolation to $t = 0$ is shown in the inset, for the sample with $x = 6.94$ in two orientations.

H. Penetration depth eigenvalues and anisotropy parameter γ

In uniaxial materials the penetration depth is a tensor with two independent eigenvalues denoted by λ_{ab} and λ_c. We define λ_i as depth of field penetration screened by supercurrent flow in the ith direction. In Kogan's formalism,[27,31] λ_{ab} and λ_c are related to the effective penetration depths for $H \| c$ and $H \| ab$ according to the following relations:

$$\lambda_{\rm eff}(H \| c) = \lambda_{ab}, \quad \lambda_{\rm eff}(H \| ab) = \sqrt{\lambda_{ab}\lambda_c} \ . \tag{8}$$

Using the $M \sim \ln H$ analysis with a BCS clean-limit temperature dependence for $\lambda(T)$ as already described, we determined $\lambda_{\rm eff}(0)$ with $H \| ab$ for the samples $x = 6.94$ and $x = 6.85$, obtaining 383 and 532 nm, respectively. Combining these results with values for $\lambda_{ab}(0)$ (obtained from studies with $H \| c$) gives $\lambda_c(0)$ values of 853 and 1210 nm, respectively. The anisotropy parameter is then $\gamma = \lambda_c/\lambda_{ab}$, which is related to the components of the normalized mass tensor m_i (with $i = 1, 3$) as follows:

$$\gamma^2 = m_3/m_1 = m_1^{-3} = m_3^{3/2} \quad \text{with } m_1^2 m_3 = 1 \ . \tag{9}$$

From the λ eigenvalues we found $\gamma = 4.96$ for the $x = 6.94$ sample and $\gamma = 5.17$ for the $x = 6.85$ sample. The similarity of these results suggests that the intrinsic superconducting mass anisotropy of Y 1:2:3 was not significantly affected by oxygen deficiency.

This analysis yielded an effective mass ratio m_3/m_1 near 25. However, this finding is depressed somewhat from the "true" value due to misalignments of some crystallites in our sample. Indeed, the x-ray rocking curve possessed a full-width at half maximum (FWHM) of 7°. So, the magnetization M actually measured contained contributions of crystallites whose c axes were distributed in a cone of about 7° width about the field direction. With $H \| c$, the angularly averaged M is slightly smaller than ideal, while with $H \| ab$ it is greater than ideal. The influence of misalignment is more severe for the latter case.

Using the angular dependence,[27] and assuming the distribution of orientations to be either Gaussian or Lorentzian, we calculated the mean-parallel magnetization relative to its value for perfect alignment, M_p/M_0. This correction increased γ from 5.0 to 5.4 if a Gaussian distribution was assumed, and to 8 if a Lorentzian distribution was assumed. Since the x-ray rocking curve was more nearly Gaussian, we conclude that the "true" value

of effective mass ratio m_3/m_1 for these Y 1:2:3 samples lies near 30 (instead of 25), in good agreement with results reported by other workers.[21,31]

It is worth mentioning here that the full analysis was used to study $H\|ab$ magnetization versus field data on one sample ($x=6.85$), following identical procedure as with $H\|c$ orientation. According to the analysis, the additional (and legitimate) condition that $F_c(0)$ be the same in both cases could be fulfilled only if $\kappa_{H\|ab}\approx 400$ (as compared with $\kappa_{H\|c}\approx 72$). Since $\kappa=H_{c2}/\sqrt{2}\,H_c$ and H_c does not change, the ratio of the two κ's gives the anisotropy parameter $\gamma=\xi_{ab}/\xi_c\approx 5.6$, corroborating our previous finding.

IV. DISCUSSION

Overall, the experimental data were reproducible and internally consistent. Most of the measurements were done in a high dc magnetic field, which thoroughly decouples the relatively weak intergrain connectivity of the polycrystalline sample. The results exhibit a smooth variation with oxygen content, and excellent agreement at full oxygenation with accepted findings on single crystals and aligned material. Therefore we are confident of the overall validity of the present results. Many questions remain open for discussion and additional questions arise. We will address some of them here.

A. Secondary maxima of J_c

The origin of the J_c maxima in Y 1:2:3 crystals has been attributed to oxygen inhomogeneities and internal granularity.[2] It is remarkable therefore that our fully oxygenated sample ($x=7.00$) still shows anomalous magnetization at high temperatures. This may be due to residual oxygen inhomogeneities or to impurities in the material, rendering the sample "granular," with regions of depressed T_c and H_{c2}. According to this interpretation, at low fields all regions are superconductive and J_c is due to the usual crystal defects. As H exceeds the upper critical field of the depressed regions, these are driven normal and become additional pinning sites, with the consequent increase in J_c. Secondary maxima of J_c occur when all depressed regions are driven normal. At higher fields, the decline of J_c with H reflects the usual and expected weakening of the pinning strength, with all the pinning sites active. No anomaly is observed in the magnetic hysteresis with $H\|ab$, as reported above, because the upper critical fields of the depressed regions with $H\|ab$ are perhaps too high, out of the observation range. In this orientation, strong "intrinsic" pinning[33] by the layered structure also inhibits vortex motion in a direction normal to the CuO layers.

The downward shift in the positions of the J_c maxima with δ (Fig. 5) can be understood in this model in the following way: the removal of oxygen debilitates not only the superconducting matrix but also reduces T_c and H_{c2} of the depressed regions. Hence, the field value at which all depressed regions are driven normal decreases, and the positions of the J_c maxima shift down.

There was in our findings no evidence of steep fall in the magnetic hysteresis for fields beyond the maxima, which has been suggested as indicative of O-deficient regions linking up at higher fields and inducing intragrain granularity in single crystals.[2] Apparently, in bulk samples, this assumption is not needed. The effect of residual oxygen inhomogeneities might be tested in future experiments, if magnetically aligned samples with known average O content but inhomogeneous oxygenation could be reproducibly formed.

B. Pinning model for J_c

Let us assume a simple single site, pinning model (with $H\|c$ and $B=$ flux density) in which the pinning force density $F_p=J_cB$ can be computed as the gradient of the pinning energy (related to the condensation energy) per vortex bundle ($-\nabla F_{c\phi}$) divided by the volume per bundle V_ϕ:

$$F_p=-\eta|\nabla F_{c\phi}|/V_\phi\ , \tag{10}$$

where $\eta\le 1$ is a numeric factor accounting for incomplete suppression of the order parameter at the pinning site and similar other deviations from the optimal case.

If the vortices are widely spaced, so that the average separation between them (or two-dimensional fluxon lattice constant "a") is larger than the average transverse separation "d" of pinning centers, the volume per bundle is $V_\phi=\tau a^2$ (where τ is the lesser of the sample thickness or a longitudinal correlation length). Approximating $\nabla F_{c\phi}$ by F_c/ξ_{ab}, the above expression becomes then

$$J_cB\approx\eta F_c(\pi l\xi_{ab}^2)/(\xi_{ab}\tau a^2)\ . \tag{11}$$

Here l is the length of the bundle actually pinned ($\ge\xi_c$). Since $B=\phi_0/a^2$ (with $\phi_0=$ flux quantum), one gets simply for J_c the model relation

$$J_c\approx\eta F_c\xi_{ab}(\tau l/\tau\phi_0)\ . \tag{12}$$

If instead the vortices are tightly packed, the average separation between flux bundles is given essentially by the average transverse separation between pinning sites; hence, the volume per bundle is $V_\phi=\tau d^2$ and the expression for J_c becomes

$$J_c\approx\eta F_c\xi_{ab}(\pi l/B\tau d^2)\ . \tag{13}$$

In either case we expect a linear relation between $J_c(0)$ and the product $F_c\xi_{ab}$ evaluated at $T=0$. Here we have assumed that the number density of effective pinning sites (and therefore d) is not changed by variations of oxygen content, which is consistent with the idea that preexisting pins are developed during solid-state reaction and initial synthesis. If then the dominant effect of oxygen depletion is to change F_c and ξ_{ab}, we should find that $J_c(0,\delta)$ varies linearly with the product $F_c(\delta)\xi_{ab}(\delta)$. This relationship is plotted in Fig. 12, which shows a convincing proportionality between the two quantities and supports the essential validity of the above model.

Previous experiments on single crystals[2] reported increased pinning for less oxygenated sample. This finding can be reconciled with the above model since in high

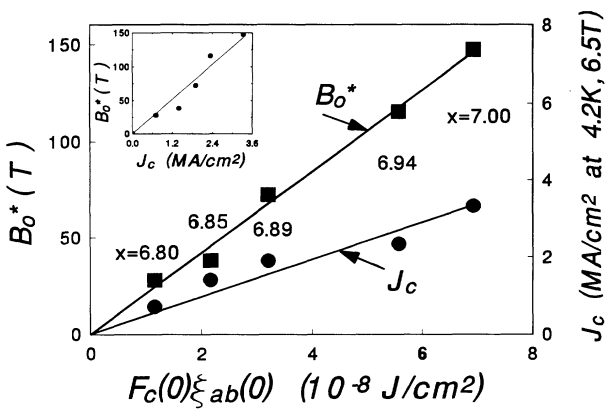

FIG. 12. The critical current density J_c and the irreversibility field B_0^* are directly related to the product $F_c(0)\xi_{ab}(0)$, as predicted by the simple pinning model discussed in the text. The resulting correlation between J_c and B_0^* is shown in the inset.

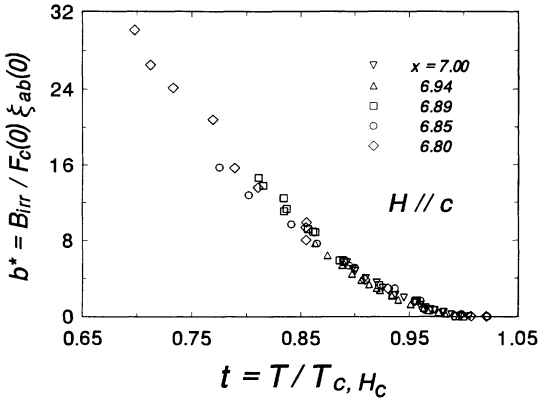

FIG. 13. The measured irreversibility lines, normalized according to the proposed pinning model, collapse to a single "universal" curve. This strongly suggests that the irreversibility line arises from vortex depinning and is actually a "depinning" line (Ref. 35).

quality single crystals the preexisting flux pinning is much weaker than in sintered material, so that a significant increase in the number of weak, oxygen-vacancy pins may offset the macroscopic electronic effects of oxygen deficiency on the pinning strength.

As noted earlier, the irreversibility field B_{irr}, extrapolated to $T=0$, is well correlated with the critical current density at low temperature. This is illustrated in the inset to Fig. 12, which plots B_0^* versus J_c at 4.2 K in a field of 6.5 T. In this range, J_c is nearly independent of field and temperature and gives an experimental measure of the total pinning, with minimal influence of thermally activated flux creep. The correlation is quite evident.

Even more convincing is the direct, linear dependence of B_0^* on the model parameter $F_c(0)\xi_{ab}(0)$, shown also in Fig. 12. This provides clear evidence that the irreversibility line (and J_c) depends on the pinning strength, which was modified via the oxygen content x.

C. Irreversibility line and "depinning"

The striking correlation of B_0^* with the pinning parameter $F_c(0)\xi_{ab}(0)$ for all five oxygen compositions investigated (linear correlation coefficient $\rho^2=0.995$) allowed us to normalize the irreversibility field by this parameter and plot the irreversibility lines in the b-t plane, where $b=B_{irr}(t)/F_c(0)\xi_{ab}(0)$ is the normalized field and t is the reduced temperature $T/T_{c,H_c}$. All five curves collapsed well into one "universal" curve, as illustrated in Fig. 13. The best scaling of temperature was obtained with the values T_{c,H_c} instead of T_c. It is clear, then, that the appropriate T_c parameter in this case is not the zero-onset value but the extrapolated value of T_c as obtained from the H_{c2} full analysis. The different choice of T_c did not affect the above correlation of B_0^* and $F_c(0)\xi_{ab}(0)$ since neither was modified.

We also tested the proposition of Guimpel *et al.*[34] that the irreversibility field B_{irr} scales with $H_{c2}(0)$, as studies in superconducting $LiTi_2O_4$ ceramic oxides prepared by different techniques seemed to indicate. Although the correlation of the curve parameter B_0^* with $H_{c2}(0)$ was fairly good, our findings indicate that the irreversibility field scales better with $F_c(0)\xi_{ab}(0)$, that is, with $[H_{c2}(0)]^{3/2}[\kappa(0)]^2$, rather than with $H_{c2}(0)$. Our results, supported by the above pinning model, favor models based on depinning rather than models based solely on intrinsic properties. In this sense, our finding strongly suggests that the irreversibility line actually is a "depinning line," as proposed by Brandt.[35]

D. Anisotropy parameter γ

As oxygen is depleted from Y 1:2:3, most superconductive properties, including the critical fields H_c, H_{c1}, and H_{c2} and associated lengths ξ and λ, change continuously and monotonically. The major exception is the transition temperature T_c, which remains nearly constant in its "plateau" for $\delta \leq 0.11$. It is noteworthy, then, that the mass anisotropy parameter $\gamma \approx 5.5$ remains nearly constant over the range of this study. Within experimental error, the same value has been obtained in earlier determinations on single crystals[21] and on magnetically aligned, isolated Y 1:2:3 powders.[36] In addition, Vandervoort *et al.*[3] have recently reported H_{c2} measurements on an oxygen-depleted Y 1:2:3 single crystal ($T_c=60$ K) and obtained the value $\gamma \approx 4.4$. While the agreement is not perfect, these results taken together indicate that the mass anisotropy undergoes relatively minor changes with oxygen deficiency even as other parameters, e.g., the condensation energy F_c, may be modified quite markedly. Since the primary effect of vacancies on chain sites (acting as a charge reservoir) is to modify the mobile charge carrier density in the CuO_2 planes, little or no change in anisotropy is expected as the factors dominating anisotropy, e.g., number and spacing of CuO_2 planes and overall crystal structure, are barely affected by formation of chain-site oxygen vacancies.

E. Condensation energy $F_c(\delta)$

Finally we want to address one of the main results of this study, namely, the sharp decrease of the condensation energy F_c with oxygen deficiency δ in the range $\delta < 0.2$, where T_c changes relatively little (especially for $\delta < 0.12$, or "90-K plateau").

Applying BCS theory, we have $F_c = N(0)\Delta(0)^2/2$, where $N(0)$ is the density of electronic states at the Fermi surface with one spin direction and $\Delta(0)$ is the superconducting energy gap at $T=0$. Replacing Δ with the gap ratio $z \equiv 2\Delta/k_B T_c$ gives $F_c \sim N(0) z^2 T_c^2$. *Assuming* that these simple relations apply to the Y 1:2:3 material, the observed decrease in F_c with δ, while T_c remains approximately constant, can occur via changes in the gap ratio and in the density of states $N(0)$. In fact, Hall effect measurements of Jones *et al.*[37] on thin epitaxial films of $YBa_2Cu_3O_{7-\delta}$ showed that the Hall carrier density decreases by a factor of ~ 2 in the T_c-plateau region relative to the density at maximum oxygenation, suggesting similar decreases in $N(0)$. This finding is fully consistent with our penetration depth determinations. Further decreases in carrier density were found at higher oxygen depletions, with a reduction of ~ 3 at a composition near $x = 6.7$. Combining this factor with the reduction in T_c measured in this study for our most depleted sample gives already a fivefold reduction in condensation energy, compared with the experimentally observed factor of ~ 11. One can speculate that the energy gap ratio z also diminishes as oxygen is removed from the superconductor. For example, a decrease of z from 7, an average value quoted for fully oxygenated Y 1:2:3, to $z \approx 4.5$ would account completely for the observed decrease of F_c. Thus, within a BCS framework, the variation of $N(0)$, $2\Delta(0)/k_B T_c$, and T_c can provide a plausible explanation for the large change in condensation energy.

Unfortunately, measurements of the gap in this and most families of high-T_c superconductors have been controversial and difficult to interpret. Along with being anisotropic, the deduced temperature dependence of $\Delta(T)$ also appears to deviate significantly from a BCS dependence, with suggestions that the observed superconductive transition may be depressed considerably below the "true" T_c by some unknown mechanism such as spin-flip scattering.[38] Therefore, we much prefer to invert the argument, as the condensation energy is an equilibrium, thermodynamic property, based upon Ginzburg-Landau theory that is independent of any specific model or mechanism for superconductivity. Our data show that in the composition range $\delta < 0.12$, where the 90-K T_c plateau is observed, the condensation energy and most of the superconductive properties vary; so it may be speculated that the constancy of T_c in this range is the anomalous property in oxygen-deficient $YBa_2Cu_3O_{7-\delta}$ which requires an explanation.[39]

V. CONCLUSIONS

This study shows that chain-site oxygen defects are not strong, effective pinning centers in the sintered $YBa_2Cu_3O_{7-\delta}$ materials investigated. In general, J_c was maximal at full oxygenation and decreased continuously as oxygen was removed (with $0 \le \delta \le 0.2$). As J_c decreased, also the irreversibility field B_{irr} was depressed. Both J_c and the parameter B_0^* of the irreversibility line showed good correlation with the pinning model parameter $F_c(0)\xi_{ab}(0)$, where *all* quantities were determined experimentally as a function of oxygen content. The condensation energy and, thus, the energy barrier of the preexisting pinning centers, were adversely affected with oxygen deficiency. The addition of chain-site oxygen vacancies, which may act as additional pinning centers, did not compensate for the weakening of the pinning strength of the preexisting defects and it had, indeed, the effect of hindering the intragrain current-carrying capacity of sintered $YBa_2Cu_3O_{7-\delta}$.

Note added in proof. Vanacken *et al.*[40] have recently reported a correlation between B_0^* and $J_c(0)$, similar to that discussed in Sec. IV. No experimental evidence was given for the origin of this correlation.

ACKNOWLEDGMENTS

The authors would like to thank R. Feenstra and D. P. Norton for useful comments and discussions. A portion of the work of J.R.T. and Y.R.S. was supported by the Science Alliance at The University of Tennessee, Knoxville. Research was sponsored by the Division of Materials Sciences, U.S. Department of Energy, and technology development was funded by the Oak Ridge Superconducting Technology for Electric Energy Systems Program, Advanced Utility Concepts Division, Conservation, and Renewable Energy Program, U.S. Department of Energy, both under Contract No. DE-AC-05-84OR21400 with Martin Marietta Energy Systems, Inc.

*Present address: Universidad de Talca, Talca, Chile.

[1] J. E. Tkaczyk and K. W. Lay, J. Mater. Res. **5**, 1368 (1990).

[2] M. Daeumling, J. M. Seuntjens, and D. C. Larbalestier, Nature (London) **346**, 332 (1990).

[3] K. G. Vandervoort, U. Welp, J. E. Kessler, H. Claus, G. W. Crabtree, W. K. Kwok, A. Umezawa, B. W. Veal, J. W. Downey, A. P. Paulikas, and J. Z. Liu, Phys. Rev. B **43**, 13 042 (1991).

[4] R. Feenstra, D. K. Christen, C. E. Klabunde, and J. D. Budai, Phys. Rev. B **45**, 7555 (1992).

[5] D. K. Christen and R. Feenstra, Physica C **185-189**, 2225 (1991).

[6] B. M. Lairson, J. L. Vargas, S. K. Streiffer, D. C. Larbalestier, and J. C. Bravman, in Proceedings of the Third International Conference on Materials and Mechanisms of Superconductivity, Kanazawa, Japan, 1991 [Physica C **185-189**, 2161

(1991)].
[7]H. Theuss and H. Kronmüller, Physica C **177**, 253 (1991).
[8]An overview on oxygen effects can be found in *Oxygen Disorder Effects in High-T_c Superconductors,* edited by J. L. Moran-Lopez and I. K. Schuller (Plenum, New York, 1990).
[9]T. B. Lindemer, J. F. Hunley, J. E. Gates, A. L. Sutton, J. Brynestad, C. R. Hubbard, and P. K. Gallagher, J. Am. Ceram. Soc. **72**, 1775 (1989).
[10]R. G. Cava, B. Batlogg, C. H. Chen, E. A. Rietman, S. M. Zahurak, and D. Werder, Phys. Rev. B **36**, 5719 (1987).
[11]D. C. Johnston, A. J. Jacobson, J. M. Newsam, J. T. Lewandowski, D. P. Goshorn, D. Xie, and W. B. Yelon, in *Chemistry of High-Temperature Superconductors,* edited by D. L. Nelson, M. S. Whittingham, and T. F. George, ACS Symposium Series, No. 351 (American Chemical Society, Washington, D.C., 1987), p. 136.
[12]W. E. Farneth, R. K. Bordia, E. M. McCarron III, M. K. Crawford, and R. B. Flippen, Solid State Commun. **66**, 953 (1988).
[13]A. J. Jacobson, J. M. Newsam, D. C. Johnston, D. P. Goshorn, J. T. Lewandowski, and M. S. Alvarez, Phys. Rev. B **39**, 254 (1989).
[14]J. R. Thompson, D. K. Christen, H. R. Kerchner, L. A. Boatner, B. C. Sales, B. C. Chakoumakos, H. Hsu, J. Brynestad, D. M. Kroeger, J. W. Williams, Yang Ren Sun, Y. C. Kim, J. G. Ossandon, A. P. Malozemoff, L. Civale, A. D. Marwick, T. K. Worthington, L. Krusin-Elbaum, and F. Holtzberg, in *Magnetic Susceptibility of Superconductors and Other Spin Systems,* edited by T. Francavilla, R. A. Hein, and D. Liebenburg (Plenum, New York, in press).
[15]J. R. Thompson, Y. R. Sun, and F. Holtzberg, Phys. Rev. B **44**, 458 (1991).
[16]C. P. Bean, Phys. Rev. Lett. **8**, 250 (1962).
[17]A. M. Campbell and J. E. Evetts, Adv. Phys. **21**, 199 (1972).
[18]J. R. Clem and V. G. Kogan, Jpn. J. Appl. Phys. **26**, 1162 (1987).
[19]Strictly speaking, instead of R the appropriate quantity in this formula should be the weighted average over the particle size distribution $\langle R \rangle \equiv \langle R^4 \rangle / \langle R^3 \rangle$ [Y. C. Kim, Ph.D. thesis, University of Tennessee, May 1989, pp. 158–160; D. K. Christen *et al.*, IEEE Trans. Magn. **25**, 2324 (1989)].
[20]Ch. Neumann, Ch. Heinzel, P. Ziemann, K. Fischer, and W. Gawalek, Z. Phys. B **84**, 37 (1991).
[21]U. Welp, W. K. Kwok, G. W. Crabtree, K. Vandervoort, A. Umezawa, and J. Z. Liu, Phys. Rev. Lett. **62**, 1908 (1989).
[22]Z. Hao, J. Clem, M. McElfresh, L. Civale, A. Malozemoff, and F. Holtzberg, Phys. Rev. B **43**, 2844 (1991).
[23]N. R. Werthamer, E. Helfand, and P. C. Hohenberg, Phys. Rev. **147**, 295 (1966).
[24]A. Abrikosov, Zh. Eksp. Teor. Fiz. **32**, 1442 (1957) [Sov. Phys. JETP **5**, 1174 (1957)].
[25]J. R. Clem, Ann. Phys. (N.Y.) **40**, 268 (1966).
[26]R. D. Parks, *Superconductivity* (Marcel Dekker, New York, 1969).
[27]V. G. Kogan, M. M. Fang, and S. Mitra, Phys. Rev. B **38**, 11 958 (1988).
[28]L. Krusin-Elbaum, R. L. Greene, F. Holtzberg, A. P. Malozemoff, and Y. Yeshurun, Phys. Rev. Lett. **62**, 217 (1989).
[29]J. R. Thompson, D. K. Christen, H. A. Deeds, Y. C. Kim, J. Brynestad, S. T. Sekula, and J. Budai, Phys. Rev. B **41**, 7293 (1990).
[30]J. R. Thompson, D. K. Christen, H. A. Deeds, Y. C. Kim, J. Brynestad, S. T. Sekula, J. Budai, and J. G. Ossandon, in *High Temperature Superconductors: Fundamental Properties and Novel Materials Processing,* edited by D. K. Christen, J. Narayan, and L. F. Schneemeyer (Materials Research Society, Pittsburgh, 1990), pp. 1065–1068.
[31]S. Mitra, J. H. Cho, W. C. Lee, D. C. Johnston, and V. G. Kogan, Phys. Rev. B **40**, 2674 (1989).
[32]Z. Hao and J. R. Clem, Phys. Rev. Lett. **67**, 2371 (1991).
[33]M. Tachiki and S. Takahashi, Solid State Commun. **70**, 291 (1989).
[34]J. Guimpel, P. Høghøj, I. Schuller, J. Vanacken, and Y. Bruynseraede, Physica C **175**, 197 (1991).
[35]E. H. Brandt, Int. J. Mod. Phys. B **5**, 751 (1991).
[36]D. E. Farrell, C. M. Williams, S. A. Wolf, N. P. Bansal, and V. G. Kogan, Phys. Rev. Lett. **61**, 2805 (1988).
[37]E. C. Jones *et al.*, private communication.
[38]R. C. Dynes (unpublished).
[39]Similar sharp reductions in F_c with δ have been reported by M. Daeumling from studies in random polycrystalline $YBa_2Cu_3O_{7-\delta}$, including materials in the 90-K T_c-plateau: Physica C **183**, 293 (1991).
[40]J. Vanacken, E. Osquiguil, and Y. Bruyneserade, Physica C **183**, 163 (1991).